Rates of Heme Oxidation and Reduction in Ru(His33)cytochrome *c* at Very High Driving Forces

Gary A. Mines, Morten J. Bjerrum,[†] Michael G. Hill,[‡] Danilo R. Casimiro,[§] I-Jy Chang,[⊥] Jay R. Winkler,* and Harry B. Gray*

Contribution from the Beckman Institute, California Institute of Technology, Pasadena, California 91125

Received June 12, 1995[⊗]

Abstract: The rates of Ru(His33)cytochrome *c* electron-transfer (ET) reactions have been measured over a driving-force range of 0.59 to 1.89 eV. The driving-force dependence of $Fe^{2+} \rightarrow Ru^{3+}$ ET in RuL_2(im)(His33)cyt *c* [L = 2,2′-bipyridine (bpy), 4,4′,5,5′-tetramethyl-2,2′-bipyridine (4,4′,5,5′-$(CH_3)_4$-bpy), 4,4′-dimethyl-2,2′-bipyridine (4,4′-$(CH_3)_2$-bpy), 4,4′-bis(*N*-ethylcarbamoyl)-2,2′-bipyridine (4,4′-$(CONH(C_2H_5))_2$-bpy), 1,10-phenanthroline (phen); im = imidazole] is well described by semiclassical ET theory with $k_{max} = 2.7 \times 10^6\ s^{-1}$ ($H_{AB} = 0.095\ cm^{-1}$) and $\lambda =$ 0.74 eV. As predicted by theory, the rate of an exergonic ($-\Delta G° = 1.3$ eV) heme reduction reaction, $*Ru^{2+}(bpy)_2$-(im)(His) → Fe^{3+}, falls in the inverted region ($k = 2.0 \times 10^5\ s^{-1}$). In contrast, the rates of three highly exergonic heme reductions, $*Ru^{2+}(phen)_2(CN)$(His) → Fe^{3+} ($2.0 \times 10^5\ s^{-1}$; 1.40 eV), $Ru^{+}(4,4'$-$(CONH(C_2H_5))_2$-$bpy)_2$(im)-(His) → Fe^{3+} ($2.3 \times 10^5\ s^{-1}$; 1.44 eV), and $Ru^{+}(phen)_2(CN)$(His) → Fe^{3+} ($4.5 \times 10^5\ s^{-1}$; 1.89 eV), are much higher than expected for reactions directly to ground-state products. Agreement with theory is greatly improved by assuming that an electronically excited ferroheme ($Fe^{2+} \rightarrow *Fe^{2+}$; ∼ 1.05 eV) is the initial product in each of these reactions.

Introduction

According to semiclassical theory, electron-transfer (ET) rates should exhibit a Gaussian dependence on the reaction driving force ($-\Delta G°$); at the optimum driving force, $-\Delta G° = \lambda$ (λ is the nuclear reorganization energy), the rate is fixed by the donor−acceptor electronic coupling (H_{AB}) (eq 1):[1]

$$k_{ET} = (4\pi^3/h^2\lambda k_b T)^{1/2}(H_{AB})^2 \exp[-(\Delta G° + \lambda)^2/4\lambda k_b T] \quad (1)$$

In the region of driving forces greater than λ (the inverted region), ET rates are predicted to decrease with increasing driving force (the inverted effect). Experimental verification of the inverted effect has come from extensive investigations of ET reactions involving both organic[2−8] and inorganic[9−14] molecules.

Owing to our interest in biological ET processes,[15] we would like to establish experimentally the magnitudes of inverted effects in proteins and other biomolecules. Some work in this area has been done,[15−23] but no single study has involved a driving-force range sufficiently wide to probe behavior far in the inverted region. We have now measured the rates of cytochrome *c* (cyt *c*) ET reactions whose driving forces vary from 0.54 to 1.89 eV. We see inverted behavior, but it is limited; at the highest driving forces, the ET reactions are much faster than expected.

Results and Discussion

We have examined three different ET processes in closely related RuL_2(X)(His33)cyt *c* molecules (Table 1). $Fe^{2+} \rightarrow Ru^{3+}$ ET ($^{O}k_{ET}$) was measured using an oxidative flash-quench method

[†] Present address: Department of Chemistry, The Royal Veterinary and Agricultural University, Frederiksberg, Denmark DK-1871.
[‡] Present address: Department of Chemistry, Occidental College, Los Angeles, CA 90041.
[§] Present address: The Scripps Research Institute, La Jolla, CA 92037.
[⊥] Present address: Department of Chemistry, National Taiwan Normal University, Taipei, Taiwan 117.
[⊗] Abstract published in *Advance ACS Abstracts,* February 1, 1996.

(1) Marcus, R. A.; Sutin, N. *Biochim. Biophys. Acta* **1985**, *811*, 265−322.
(2) Miller, J. R.; Calcaterra, L. T.; Closs, G. L. *J. Am. Chem. Soc.* **1984**, *106*, 3047−3049. Closs, G. L.; Miller, J. R. *Science* **1988**, *240*, 440−447.
(3) Wasielewski, M. R.; Niemczyk, M. P.; Svec, W. A.; Pewitt, E. B. *J. Am. Chem. Soc.* **1985**, *107*, 1080−1082.
(4) Gould, I. R.; Moser, J. E.; Armitage, B.; Farid, S. J. *J. Am. Chem. Soc.* **1989**, *111*, 1917−1919.
(5) Levin, P. P.; Pluzhnikov, P. F.; Kuzmin, V. A. *Chem. Phys.* **1989**, *137*, 331−344.
(6) Irvine, M. P.; Harrison, R. J.; Beddard, G. S.; Leighton, P.; Sanders, J. K. M. *Chem. Phys.* **1986**, *104*, 315−324.
(7) Grampp, G.; Hetz, G. *Ber. Bunsenges. Phys. Chem.* **1992**, *96*, 198−200.
(8) Beitz, J. V.; Miller, J. R. *J. Chem. Phys.* **1979**, *71*, 4579−4595.
(9) Fox, L. S.; Kozik, M.; Winkler, J. R.; Gray, H. B. *Science* **1990**, *247*, 1069−1071.
(10) Chen, P.; Duesing, R.; Tapolsky, G.; Meyer, T. J. *J. Am. Chem. Soc.* **1989**, *111*, 8305−8306.
(11) Yonemoto, E. H.; Riley, R. L.; Kim, Y. I.; Atherton, S. J.; Schmehl, R. H.; Mallouk, T. E. *J. Am. Chem. Soc.* **1992**, *114*, 8081−8087.
(12) Ohno, T.; Yoshimura, A.; Mataga, N. *J. Phys. Chem.* **1986**, *90*, 3295−3297.
(13) MacQueen, D. B.; Schanze, K. S. *J. Am. Chem. Soc.* **1991**, *113*, 7470−7479.
(14) McCleskey, T. M.; Winkler, J. R.; Gray, H. B. *J. Am. Chem. Soc.* **1992**, *114*, 6935−6937. McCleskey, T. M.; Winkler, J. R.; Gray, H. B. *Inorg. Chim. Acta* **1994**, *225*, 319−322.
(15) Winkler, J. R.; Gray, H. B. *Chem. Rev.* **1992**, *92*, 369−379. Bjerrum, M. J.; Casimiro, D. R.; Chang, I-J.; Di Bilio, A. J.; Gray, H. B.; Hill, M. G.; Langen, R.; Mines, G. A.; Skov, L. K.; Winkler, J. W.; Wuttke, D. S. *J. Bioenerg. Biomembr.* **1995**, *27*, 295−302.
(16) McLendon, G.; Hake, R. *Chem. Rev.* **1992**, *92*, 481−490.
(17) Simmons, J.; McLendon, G.; Qiao, T. *J. Am. Chem. Soc.* **1993**, *115*, 4889−4890.
(18) Zhou, J. S.; Rodgers, M. A. *J. Am. Chem. Soc.* **1991**, *113*, 7728−7734.
(19) Scott, J. R.; Willie, A.; McLean, M.; Stayton, P. S.; Sligar, S. G.; Durham, B.; Millett, F. *J. Am. Chem. Soc.* **1993**, *115*, 6820−6824.
(20) Gunner, M. R.; Robertson, D. E.; Dutton, P. L. *J. Phys. Chem.* **1986**, *90*, 3783−3795.
(21) Brooks, H. B.; Davidson, V. L. *J. Am. Chem. Soc.* **1994**, *116*, 11201−11202.
(22) Lin, X.; Williams, J. C.; Allen, J. P.; Mathis, P. *Biochemistry* **1994**, *33*, 13517−13523.
(23) Jia, Y.; DiMagno, T. J.; Chan, C-K.; Wang, Z.; Du, M.; Hanson, D. K.; Schiffer, M.; Norris, J. R.; Fleming, G. R.; Popov, M. S. *J. Phys. Chem.* **1993**, *97*, 13180−13191.

0002-7863/96/1518-1961$12.00/0

Table 1. Rate Constants and Driving Forces for Intramolecular ET in $RuL_2(X)(His33)$cytochrome *c*

complex	reaction	k_{ET} (s^{-1})	$-\Delta G°$ (eV)[a]
$Ru(4,4',5,5'\text{-}(CH_3)_4\text{-bpy})_2(im)(His)^{2+}$ (**I**)	$Fe^{2+} \rightarrow Ru^{3+}$	$1.6(2) \times 10^6$	0.54
$Ru(4,4'\text{-}(CH_3)_2\text{-bpy})_2(im)(His)^{2+}$ (**II**)	$Fe^{2+} \rightarrow Ru^{3+}$	$2.0(2) \times 10^6$	0.70
$Ru(phen)_2(im)(His)^{2+}$ (**III**)	$Fe^{2+} \rightarrow Ru^{3+}$	$3.5(4) \times 10^6$	0.75
$Ru(phen)_2(CN)(His)^{+}$ (**IV**)	$Fe^{2+} \rightarrow Ru^{3+}$	$1.0(1) \times 10^7$	0.78
$Ru(bpy)_2(im)(His)^{2+}$ (**V**)	$Fe^{2+} \rightarrow Ru^{3+}$	$2.6(3) \times 10^6$	0.81
$Ru(4,4'\text{-}(CONH(C_2H_5))_2\text{-bpy})_2(im)(His)^{2+}$ (**VI**)	$Fe^{2+} \rightarrow Ru^{3+}$	$1.1(1) \times 10^6$	1.00
$Ru(bpy)_2(im)(His)^{2+}$ (**V**)	$*Ru^{2+} \rightarrow Fe^{3+}$	$2.0(5) \times 10^5$	1.3
$Ru(phen)_2(CN)(His)^{+}$ (**IV**)	$*Ru^{2+} \rightarrow Fe^{3+}$	$2.0(5) \times 10^5$	1.4 [0.35][b]
$Ru(4,4'\text{-}(CONH(C_2H_5))_2\text{-bpy})_2(im)(His)^{2+}$ (**VI**)	$Ru^{+} \rightarrow Fe^{3+}$	$2.3(2) \times 10^5$	1.44 [0.39][b]
$Ru(phen)_2(CN)(His)^{+}$ (**IV**)	$Ru^{+} \rightarrow Fe^{3+}$	$4.5(5) \times 10^5$	1.89 [0.84][b]

[a] $E°[\text{cyt } c(Fe^{3+/2+})] = 0.26$ V *vs* NHE; $E°(Ru^{3+/2+})$[**II**, **V**] = 0.96, 1.07 V (pH 7, phosphate); $E°[Ru^{3+/2+}L_2(X)(im)]$[**I**,**III**,**IV**,**VI**] = 0.80, 1.01, 1.04, 1.26 V (pH 7, phosphate); $E_{00}(*Ru^{2+})$[**V**] = 2.1 eV (pH 7, phosphate); $E_{00}[*Ru^{2+}(phen)_2(CN)(im)] = 2.2$ eV (pH 7, phosphate); $E°[Ru^{2+/+}(4,4'\text{-}(CONH(C_2H_5))_2\text{-bpy})_2(im)_2] = -1.18$ V (acetonitrile); $E°[Ru^{2+/+}(phen)_2(CN)(im)] = -1.63$ V (acetonitrile). Errors in $E°$ values are $\leq \pm 0.03$ V. [b] Assuming formation of the ferroheme ^{3}MLCT excited state.

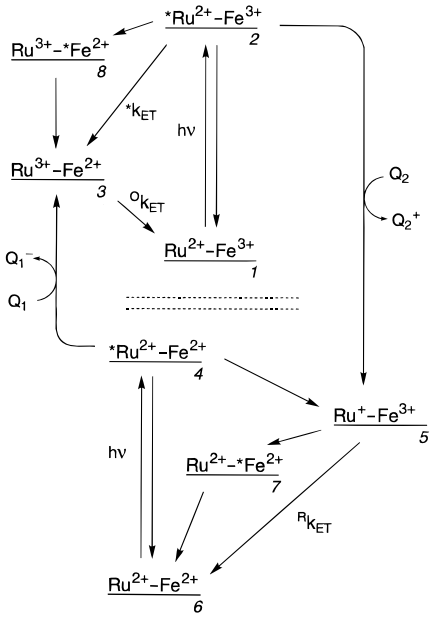

Figure 1. Reaction sequences following excitation of Ru^{2+} on oxidized (**1**) or reduced (**6**) cytochrome *c*. Ru represents the various complexes in Table 1, and Fe represents the heme group of cytochrome *c*. Q_1 is $Ru(NH_3)_6^{3+}$; Q_2 is MeODMA.

(Figure 1: **6** → **4** → **3** → **1**).[24] $*Ru^{2+} \rightarrow Fe^{3+}$ rate constants ($*k_{ET}$) were extracted by determining the yield of $Ru^{3+}-Fe^{2+}$ formed after excitation of $Ru^{2+}-Fe^{3+}$ without quencher (Figure 1: **1** → **2** → **3**). $Ru^{+} \rightarrow Fe^{3+}$ ET ($^Rk_{ET}$)[25] was measured using a reductive flash-quench procedure [Figure 1: **1** → **2** → **5** → **6**;[26] Q_2 = *p*-methoxy-*N*,*N*-dimethylaniline (MeODMA)]. Excitation of $Ru^{2+}-Fe^{3+}$ in the presence of MeODMA results in biphasic kinetics. The first phase represents loss of $*Ru^{2+}-Fe^{3+}$, accelerated by bimolecular reductive quenching [Figure 1: **2** → **5**; k_q(**IV**) ~ 6×10^8 M^{-1} s^{-1}].[27] A second kinetic phase corresponds to intramolecular reduction of the ferriheme by Ru^{+} [Figure 1: **5** → **6**; $^Rk_{ET}$(**IV**) = 4.5×10^5 s^{-1}]. Identical kinetics were observed at wavelengths sensitive to the oxidation state of the heme (385, 420, 550 nm) and the Ru complex (339, 504 nm) (Figure 2). The transient absorption spectrum just after

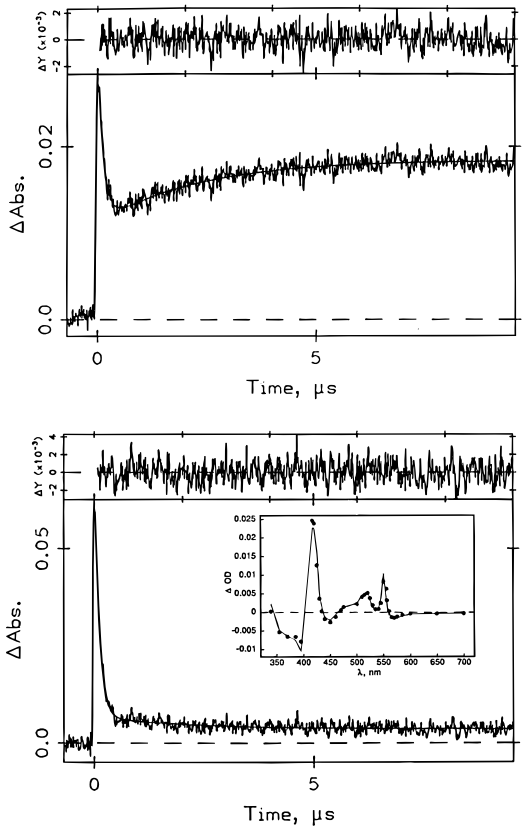

Figure 2. Transient absorption kinetics of a solution of $Ru(phen)_2$(CN)(His33)cytochrome $c(Fe^{3+})$ (18 μM) and MeODMA (9 mM) following laser flash excitation (480 nm, 20 ns, 1.9 mJ). Smooth lines are fits to a biexponential decay function; residuals are shown above each trace. The faster component corresponds to loss of $*Ru^{2+}$ (k_{obs} = 9.4×10^6 s^{-1}); the slower component corresponds to $Ru^{+} \rightarrow Fe^{3+}$ ET ($^Rk_{ET}$ = 4.5×10^5 s^{-1}). Top: Kinetics monitored at 550 nm. Bottom: Kinetics monitored at 339 nm. Inset: Transient difference spectrum (dots) observed after the slower phase (~100 μs). The solid line is the sum of the spectra of $(Fe^{2+}-Fe^{3+})$ cytochrome *c* (ref 28) and $MeODMA^{\bullet+}$ (ref 29).

the second phase accords closely with the sum of the spectra of $(Fe^{2+}-Fe^{3+})$cyt *c* and $MeODMA^{\bullet+}$ (Figure 2, inset).[28,29] On a millisecond time scale, $MeODMA^{\bullet+}$ reoxidizes the heme.[30]

Analysis of the driving-force dependence of the $Fe^{2+} \rightarrow Ru^{3+}$ reaction gives λ = 0.74 eV and H_{AB} = 0.095 cm^{-1} (Figure 3,

(24) Chang, I-J.; Gray, H. B.; Winkler, J. R. *J. Am. Chem. Soc.* **1991**, *113*, 7056−7057.

(25) "Ru^{+}" denotes the species in which ruthenium is in the +2 oxidation state and one of the ligands is a radical anion [Ru^{2+}−(diimine$^{\bullet-}$)] regardless of the overall charge on the complex.

(26) Mines, G. A.; Winkler, J. R.; Gray, H. B. *J. Inorg. Biochem.* **1993**, *51*, 236.

(27) The transient absorption spectrum immediately after the fast kinetic phase accords with the difference spectrum $(Fe^{2+}-Fe^{3+})$cyt *c*, indicating some direct intramolecular ET quenching of $*Ru^{2+}$ by Fe^{3+} followed by reductive scavenging by MeODMA.

(28) Margoliash, E.; Frohwirt, N. *Biochem. J.* **1959**, *71*, 570−572.

(29) Sassoon, R. E.; Gershuni, S.; Rabani, J. *J. Phys. Chem.* **1992**, *96*, 4692−4698.

(30) After many shots, reduced protein is observed in the steady-state absorption spectrum, indicating some irreversibility. This is most likely due to dimerization of some of the $MeODMA^{\bullet+}$ radicals.

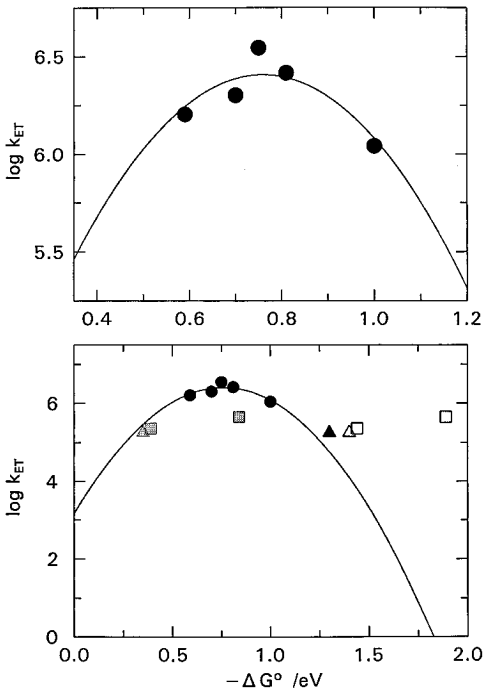

Figure 3. Driving-force ($-\Delta G°$) dependence of intramolecular ET rate constants in Ru(His33)cyt *c* (Table 1). Top: $Fe^{2+} \rightarrow Ru^{3+}$ ET in RuL_2(im)(His33)cyt *c*. The line represents the best fit to eq 1 ($H_{AB} = 0.095$ cm^{-1}; $\lambda = 0.74$ eV). Bottom: Replot of the above $k_{ET}/-\Delta G°$ curve with the addition of $Ru^{+} \rightarrow Fe^{3+}$ (rectangles) and $*Ru^{2+} \rightarrow Fe^{3+}$ (triangles) data. The open symbols represent the highly exergonic reactions directly to ground-state products; the gray symbols represent the reaction channel involving formation of the ferroheme ^{3}MLCT excited state (∼1.05 eV).

top). The Ru(phen)$_2$(CN)(His33)cyt *c* $Fe^{2+} \rightarrow Ru^{3+}$ rate constant, while consistent with the analysis, is statistically an outlier, and was not included in the fit of the RuL_2(im)(His)cyt *c* data. Cyanide binding to ruthenium evidently perturbs the Ru−heme electronic coupling relative to Ru−im ligation. Indeed, calculations indicate that the $Fe^{2+} \rightarrow Ru^{3+}$ rate constant is sensitive to the Ru orbital that provides the coupling to the bridge,[31] and experimental work shows that varying X in RuL_2(X)(His) could slightly alter the Ru−His coupling.[32]

One of the $*Ru^{2+} \rightarrow Fe^{3+}$ rates [$*k_{ET}$(**V**)] is well described by the $Fe^{2+} \rightarrow Ru^{3+}$ analysis; however, the other $*Ru^{2+} \rightarrow Fe^{3+}$ rate [$*k_{ET}$(**IV**)], as well as the $Ru^{+} \rightarrow Fe^{3+}$ rates [$^Rk_{ET}$(**IV**) and $^Rk_{ET}$(**VI**)], are higher than expected for the driving forces involved (Figure 3, bottom). In particular, $^Rk_{ET}$(**IV**) is more than six orders of magnitude higher than predicted. We can rule out variations in outer-sphere reorganization energies (λ_o) as an explanation for this anomalous rate/energy behavior: according to dielectric continuum models,[33] λ_o depends on donor−acceptor properties that do not vary significantly for the different types of ET reactions in Ru(His33)cyt *c* molecules. Electronic-coupling variations cannot explain the rate/energy behavior either. The donor electron in the $*Ru^{2+} \rightarrow Fe^{3+}$ and $Ru^{+} \rightarrow Fe^{3+}$ reactions is localized in a diimine π^* orbital. The first step in the ET pathway involves coupling to the Ru or directly to the protein. In either case, the coupling should be slightly *weaker* than that for $Fe^{2+} \rightarrow Ru^{3+}$ ET.[34] Deviations from inverted behavior involving anomalously fast inverted rates often are attributable to quantum effects: specifically, the inverted effect can be attenuated at high driving forces by nuclear tunneling along one or more coordinates of high-frequency vibrational modes.[35] We do not favor this explanation in our case, however, because an unreasonably large inner-sphere reorganization energy ($\lambda_i \sim 1$ eV) is necessary to accommodate $^Rk_{ET}$(**IV**) in the fit.[36]

It has been suggested that $Ru^{+} \rightarrow Fe^{3+}$ reactions are so exergonic that formation of an electronically excited species (at lower driving force) is faster than the (highly inverted) reaction directly to ground-state $Ru^{2+}-Fe^{2+}$.[37] Although the lowest Ru^{2+} excited states are out of reach (≥1.9 eV),[38] those for ferrocytochrome *c* are not: the origin of the transition to the ^{1}MLCT [Fe(dπ) → P(π^*), P = porphyrin] excited state is roughly 1.3 eV[39] and the ^{3}MLCT state is estimated at ∼1.05 eV.[40] Indeed, the rates predicted for the $Ru^{+}-Fe^{3+} \rightarrow Ru^{2+}-*Fe^{2+}$(^{3}MLCT) reactions of complexes **VI** and **IV** (Figure 1: **5** → **7**) are close to those observed for $Ru^{+} \rightarrow Fe^{3+}$ ET (Figure 3, bottom).[41] Similar analysis indicates that the $*Ru^{2+}-Fe^{3+} \rightarrow Ru^{3+}-*Fe^{2+}$(^{3}MLCT) reaction of complex **IV** (Figure 1: **2** → **8**) is faster than inverted ET directly to a ground-state ferroheme.[42,43]

The phenomenon of rate/energy leveling is common for photoinduced charge separation;[44] most examples of inverted behavior involve recombination reactions.[45] Invoking the formation of excited-state products is one explanation of rate leveling:[8,14,44,46,47] photoinduced charge separation generally produces open-shell species (radicals) possessing low-lying excited states, whereas recombination reactions yield closed-shell products.[14] A key role played by electronic structure in ET kinetics is underscored by our finding that a relatively low-lying excited state of a closed-shell product can open a noninverted decay channel deep in the inverted region—the region in which thermal (energy wasting) recombinations of photogenerated charge-separated states are usually inhibited.

(31) Stuchebrukhov, A. A.; Marcus, R. A. *J. Phys. Chem.* **1995**, *99*, 7581−7590.

(32) LaChance-Galang, K. J.; Doan, P. E.; Clarke, M. J.; Rao, U.; Yamano, A.; Hoffman, B. M. *J. Am. Chem. Soc.* **1995**, *117*, 3529−3538.

(33) Marcus, R. A. *Annu. Rev. Phys. Chem.* **1964**, *15*, 155−196. Brunschwig, B. S.; Ehrenson, S.; Sutin, N. *J. Phys. Chem.* **1986**, *90*, 3657−3668.

(34) The former case involves an additional covalent bond relative to the $Fe^{2+} \rightarrow Ru^{3+}$ pathway; the latter involves a through-space jump (van der Waals interaction) having no counterpart in the $Fe^{2+} \rightarrow Ru^{3+}$ pathway.

(35) Brunschwig, B. S.; Sutin, N. *Comments Inorg. Chem.* **1987**, *6*, 209−235.

(36) Tunneling efficiency depends on the magnitude of the distortion along the high-frequency vibrational coordinates (λ_i). The λ_i associated with $Ru^{+/2+}$(diimine) reactions should be similar to that for Ru(bpy)$_3^{2+}$ MLCT [Ru(dπ) → bpy(π^*)] excitation (0.17 eV: Sutin, N.; Brunschwig, B. S.; Creutz, C.; Winkler, J. R. *Pure Appl. Chem.* **1988**, *60*, 1817−1830).

(37) Heacock, D. H., II; Harris, M. R.; Durham, B.; Millett, F. *Inorg. Chim. Acta* **1994**, *226*, 129−135.

(38) Casimiro, D. R. Ph.D. Thesis 1994, California Institute of Technology.

(39) Eaton, W. A.; Charney, E. *J. Chem. Phys.* **1969**, *51*, 4502−4505. Makinen, M. W.; Churg, A. K. In *Iron Porphyrins, Part One*; Lever, A. B. P., Gray, H. B., Eds.; Addison-Wesley Publishing Company: Reading, 1983; pp 141−235.

(40) For comparison, the MLCT singlet−triplet gap in Fe(bpy)$_3^{2+}$ is ∼0.25 eV (Kober, E. M.; Meyer, T. J. *Inorg. Chem.* **1982**, *21*, 3967−3977).

(41) The fact that the energy-adjusted $^Rk_{ET}$(**IV**) point falls slightly below the value predicted from the $Fe^{2+} \rightarrow Ru^{3+}$ analysis may reflect the slightly weaker electronic coupling expected for $Ru^{+} \rightarrow Fe^{3+}$ reactions.

(42) Subsequent excited-state deactivation (Figure 1: **8** → **3** and **7** → **6**) should be very fast, $>10^{11}$ s^{-1} (Huppert, D.; Straub, K. D.; Rentzepis, P. M. *Proc. Natl. Acad. Sci. U.S.A.* **1977**, *74*, 4139−4143. Li, P.; Sage, J. T.; Champion, P. M. *J. Chem. Phys.* **1992**, *97*, 3214−3227).

(43) LF(Ru^{3+}) excited states also could be formed in $*Ru^{2+} \rightarrow Fe^{3+}$ ET reactions. These states, however, are at relatively low energies (∼1000 cm^{-1}; LaChance-Galang *et al.* in ref 32) and their population is not likely to significantly affect $*Ru^{2+} \rightarrow Fe^{3+}$ ET rates.

(44) Rehm, H.; Weller, A. *Isr. J. Chem.* **1970**, *8*, 256−271.

(45) Suppan, P. *Top. Curr. Chem.* **1992**, *163*, 95−130.

(46) Kikuchi, K.; Niwa, T.; Takahashi, Y.; Ikeda, H.; Miyashi, T. *J. Phys. Chem.* **1993**, *97*, 5070−5073.

(47) Siders, P.; Marcus, R. A. *J. Am. Chem. Soc.* **1981**, *103*, 748−752.

Experimental Section

General. Protein solutions were concentrated using ultrafiltration units (stirred cells or centricon devices) containing YM3 or YM10 membranes (Amicon). G-25 Sephadex (Pharmacia) was used for gel filtration chromatography, and unless otherwise specified, columns were preequilibrated and eluted with $\mu = 0.1$ sodium phosphate buffer, pH 7.0. Unless stated otherwise, cation-exchange chromatography was performed using an HR 16/10 Mono S prepacked column attached to an FPLC system (Pharmacia). Linear NaCl gradients were used for elution (loading buffer (pump A) $\mu = 0.1$ sodium phosphate, pH 7; limit buffer (pump B) 0.25 M NaCl, buffered to pH 7 using sodium phosphate (~25 mM)). Absorption spectra were measured using a Hewlett-Packard 8452A Diode-Array spectrophotometer.

Materials. Horse heart cytochrome *c* (type VI) was obtained from Sigma and was typically purified by cation-exchange chromatography (FPLC) before use. Buffers were prepared using reagent grade chemicals and distilled house water purified by passage through a Barnstead NANOpure system. 1,10-Phenanthroline (phen), 2,2′-bipyridine (bpy), 4,4′-dimethyl-2,2′-bipyridine (4,4′-$(CH_3)_2$-bpy), and imidazole (im) were purchased from either Merck or Aldrich and used as received. *p*-Methoxy-*N*,*N*-dimethylaniline (MeODMA) was obtained from *p*-methoxyaniline (TCI) by reaction with dimethyl sulfate according to a published procedure,[48] followed by room temperature sublimation under static vacuum; it was stored in the dark under argon until just prior to use. Ruthenium(III) chloride hydrate was used as received from Johnson Matthey or Aldrich. Hexaammineruthenium-(III) chloride (Aldrich) was recrystallized from warm 1 M HCl (<40 °C) before use. RuL_2Cl_2, $RuL_2(im)_2Cl_2$, and $RuL_2(CO_3)$ were prepared by literature procedures for the analogous $Ru(bpy)_2Cl_2$,[49] $Ru(bpy)_2(im)_2Cl_2$,[50] and $Ru(bpy)_2(CO_3)$[51] compounds, with minor modifications.

4,4′,5,5′-Tetramethyl-2,2′-bipyridine (4,4′,5,5′-$(CH_3)_4$-bpy).[52] 2,3-Dimethylpyridine (30 mL) was refluxed with a Pd/C catalyst (10% Pd, Aldrich) for 8 days. A solid material was obtained upon cooling. Toluene/chloroform (~1:1) was added to dissolve the solid, and the solution was filtered hot. Rotary evaporation of the filtrate yielded a white precipitate that was isolated by filtration and washed with a small amount of toluene/chloroform. Yield: 6 g. ^{1}H NMR spectrum (in DCl, pH 1, uncorrected): singlets at 8.25 (1), 7.75 (1), 2.34 (3), and 2.25 (3). The product was recrystallized from ethyl acetate.

4,4′-Bis(*N*-ethylcarbamoyl)-2,2′-bipyridine (4,4′-$(CONH(C_2H_5))_2$-bpy). 4,4′-Dicarboxy-2,2′-bipyridine[53] (3 g, 12 mmol) was refluxed in 30 mL of thionyl chloride for 3−4 h, producing a yellow solution. Excess thionyl chloride was removed under vacuum, and the resulting residue was dried at 50 °C under vacuum. Dry benzene (80 mL) was added, and treatment of the suspension with excess freshly distilled ethylamine (3 mL, 45 mmol) yielded instant precipitation of the white product. The mixture was refluxed for another hour. Chloroform (100 mL) was added to dissolve impurities, and the reaction mixture was filtered. The white solid was washed with ether and dried in air. Yield: 2.1 g. ^{1}H NMR spectrum (in 0.25 M DCl): d at 8.98 (2), s at 8.77 (2), d at 8.15 (2), q at 3.47 (4), and t at 1.24 ppm (6).

[Ru(phen)$_2$(CN)(im)]Cl. $Ru(phen)_2Cl_2$ (297 mg, 0.53 mmol), KCN (48 mg, 0.79 mmol), and im (47 mg, 0.69 mmol) were refluxed in water/ethanol (1:1) for 3 h, and the red solution was rotary-evaporated to dryness. The residue was redissolved in a minimum of water/ethanol (~5:1), and the solution was applied to a cation-exchange column preequilibrated with water (SP-Sephadex, 12 cm × 4 cm i.d.). A small amount of $Ru(phen)_2(CN)_2$ eluted in the void volume (with water). $Ru(phen)_2(CN)(im)^+$ was eluted with 0.5 M NaCl (~500 mL). The volume was reduced to ~60 mL by rotary evaporation, yielding precipitation of an orange solid. After incubation at 0 °C for 2 h, the solid was isolated by filtration, washed with ether, and air dried. ^{1}H NMR spectrum (in D_2O): d at 9.89 (1), d at 8.68 (1), d at 8.54 (1), d at 8.45 (1), d at 8.31 (1), d at 8.17 (1), d at 8.02 (1), d at 7.99 (1), m at 7.91 (3), dd at 7.81 (1), d at 7.74 (1), d at 7.70 (1), s at 7.61 (1), dd at 7.32 (1), dd at 7.16 (1), s at 6.86 (1), s at 6.64 (1).

RuL$_2$(im)(His33)cyt *c*. $Ru(bpy)_2(im)$(His33)cyt *c* was prepared according to a published procedure[54] with minor modifications. A solution of ferricytochrome *c* (0.5 mM, 15 mL; $\mu = 0.1$ phosphate buffer, pH 7.0) was stirred under Ar with $Ru(bpy)_2(CO_3)$ (36 mg, ~5 mM) for 18−24 h at room temperature in the dark. Excess $Ru(bpy)_2(H_2O)_2$ was separated by gel filtration (G-25 Sephadex, 30 cm × 2.5 cm i.d.). Solid imidazole was added to the protein fraction (to make ~1 M), and the solution sat in the dark for 1−3 days (pH unadjusted). After gel filtration to remove excess imidazole, the protein band was concentrated by ultrafiltration (Amicon) and loaded onto a Mono S column for purification by FPLC (Pharmacia). The band eluting at ~60% buffer B was concentrated, desalted by gel filtration, and purified 1−2 more times by FPLC; the absorption spectrum indicated the presence of a single $Ru(bpy)_2(im)$(His) moiety per cyt *c* (e.g., $OD_{292}/OD_{410} = 0.67$). The site of modification was determined by tryptic digestion of the modified protein, followed by purification and amino acid sequencing of the Ru-containing peptide.[38]

The other $RuL_2(im)$(His33)cyt *c* molecules were prepared as above, with the following modifications: In the preparation of Ru(4,4′,5,5′-$(CH_3)_4$-bpy)$_2$(im)(His33)cyt *c*, $Ru(4,4'5,5'\text{-}(CH_3)_4\text{-bpy})_2Cl_2$, dissolved in 100−200 μL methanol, was used instead of the carbonato complex. The modification reaction involving Ru(4,4′-$(CONH(C_2H_5))_2$-bpy)$_2$-(CO_3) used 2−3 times greater concentrations of both reagents and required 2−4 days at 30−35 °C; the subsequent imidazole reaction was conducted at 30−35 °C and pH 8.5. In the preparation of Ru-(phen)$_2$(im)(His33)cyt *c*, the modification reaction took ~2 days, and protein solutions were passed through a screening column (SP Sepharose, 3 cm × 2.5 cm i.d.; eluent: 0.25 M NaCl, pH 7) to remove multiply modified and/or other highly binding side products prior to loading on the FPLC column (the solution off the screening column was desalted by repetitive concentration/dilution cycles in an Amicon ultrafiltration cell).

Ru(phen)$_2$(CN)(His33)cyt *c*. Modification using $Ru(phen)_2(CO_3)$ was carried out as above, but after gel filtration to remove excess Ru-(phen)$_2$(H$_2$O)$_2$, the protein solution was passed through an SP Sepharose screening column (see above), and loaded on a Mono S column for purification by FPLC. The band eluting at ~60% buffer B (Ru(phen)$_2$-(H$_2$O)(His33)cyt *c*) was concentrated to ~0.7 mM, reduced with excess sodium dithionite, and passed through a gel filtration column preequilibrated and eluted with 0.2 M diethanolamine, pH 9.1. Solid KCN was added (to make 0.22 N KCN) and the solution (~0.2 mM Ru-cyt *c*) was stirred under argon in the dark for 3 days. The reaction was stopped by passage down a gel filtration column, and the protein solution was oxidized overnight at 4 °C by addition of >100-fold excess of solid KCoEDTA. The solution was then loaded onto a Mono S column, and Ru(phen)$_2$(CN)(His33)cyt *c* eluted at 45% buffer B. Numerous side products were observed, including unreacted Ru(phen)$_2$-(H$_2$O)(His33)cyt *c*, and 1−2 additional FPLC runs were necessary to achieve baseline separation.

Kinetics. Protein solutions for oxidative flash-quench measurements were reduced by excess sodium dithionite and passed through a gel filtration column just prior to each experiment. Solutions (1.5−4 mL) of 12−20 μM Ru-cyt *c* and either 3−7 mM $Ru(NH_3)_6Cl_3$ (for oxidative flash-quench experiments) or 5−9 mM MeODMA (for reductive flash-quench experiments) in $\mu = 0.1$ sodium phosphate buffer, pH 7.0, were Ar-degassed by repetitive pump/fill cycles in vacuum cells fitted with 1 cm quartz cuvette side arms. In the photoinduced experiments involving **IV**, aniline (5−25 mM) was used to scavenge Ru^{3+} in order to determine the yield of Fe^{2+}. Kinetics were monitored by transient absorption; the excitation source was a dye laser (Lambda Physik FL3002; Coumarin 480, 20 ns/pulse, 480 nm, 1−3 mJ/pulse) pumped

(48) Sekiya, M.; Tomie, M.; Leonard, N. J. *J. Org. Chem.* **1968**, *33*, 318−322.

(49) Sullivan, B. P.; Salmon, D. J.; Meyer, T. J. *Inorg. Chem.* **1978**, *17*, 3334−3341.

(50) Long, C.; Vos, J. G. *Inorg. Chim. Acta* **1984**, *89*, 125−131.

(51) Johnson, E. C.; Sullivan, B. P.; Adeyemi, S. A.; Meyer, T. J. *Inorg. Chem.* **1978**, *17*, 2211−2215.

(52) This procedure is based on a literature method for making symmetrically substituted bipyridines (Sasse, W. H. F.; Whittle, C. P. *J. Chem. Soc.* **1961**, 1347−1350).

(53) Sprintschnik, G.; Sprintschnik, H. W.; Kirsch, P. P.; Whitten, D. G. *J. Am. Chem. Soc.* **1977**, *99*, 4947−4954.

(54) Durham, B. D.; Pan, L. P.; Hahm, S.; Long, J.; Millett, F. In *ACS Advances in Chemistry Series*; Johnson, M. K., King, R. B., Kurtz, D. M., Kutal, C., Norton, M. L., Scott, R. A., Eds.; American Chemical Society: Washington, DC, 1990; Vol. 226, pp 180−193.

by a XeCl excimer laser (Lambda Physik LPX210i), and the probe source was a 75 W xenon arc lamp.

Electrochemistry. Electrochemical measurements were made using a BAS (Model 100 or Model CV-50W) electrochemical analyzer, with platinum wire as the auxiliary electrode; potentials were converted to NHE by using $E°$(SCE) = 0.241 V. $Ru^{3+/2+}$ potentials of model complexes were measured in sodium phosphate buffer ($\mu = 0.1$, pH = 7.0) by cyclic voltammetry using either a platinum or glassy carbon working electrode and SCE as the reference electrode. $Ru^{3+/2+}$ potentials of **II** and **V** were determined by Osteryoung square-wave voltammetry [potential range 0.3−1.0 V (*vs* SCE), step height 2 mV, square-wave amplitude 25 mV, frequency 5 Hz] using an edge-plane graphite electrode (5 mm diameter) as the working electrode and SCE as the reference; samples (∼1 mL) were 1−3 mM protein, $\mu = 0.1$ sodium phosphate buffer, pH = 7.0. $Ru^{2+/+}$ potentials were recorded *vs* AgCl/Ag at an edge-plane graphite electrode in acetonitrile (Burdick and Jackson) with 0.1 M tetrabutylammonium hexafluorophosphate (Southwestern Analytical) as supporting electrolyte; they were corrected for the junction potential and converted to SCE using ferrocenium/ferrocene as an internal standard.[55]

Acknowledgment. We thank Jerôme Claverie for assistance with several syntheses. G.A.M. acknowledges an NSF graduate fellowship and an NIH traineeship. M.J.B. was a Carlsberg Foundation Scholar in the Beckman Institute during 1991−1993. This work was supported by grants from NSF (CHE9214569) and NIH (DK19038).

JA9519243

(55) In our cell, cyclic voltammetry of a 0.05 mM ferrocenium nitrate solution in 1.00 M KCl gave $E°(Fc^+/Fc) = 0.139$ V *vs* SCE. Junction potentials in acetonitrile were found to be ∼150−300 mV.